EUROPEAN ORGANIZATION FOR NUCLEAR RESEARCH

Nijmegen HEN-408
L3 note 2270
June 12, 1998

A Two-Dimensional Study of Bose-Einstein Correlations in Z decays at LEP

J.A. van Dalen, S.V. Chekanov[1)], W. Kittel, W.J. Metzger
University of Nijmegen/NIKHEF

Abstract

We report on a study of Bose-Einstein correlations in Z decays at LEP with the L3 detector. The analysis is performed in two dimensions (parallel and transverse to the thrust axis) in the LCMS (longitudinally comoving system).

1) Now at Argonne National Laboratory.

1 Introduction

Bose-Einstein correlations are observed as an enhancement of the production of identical bosons at small four-momentum separation, relative to what uncorrelated production would have led to [1]. For a review see e.g. [2].

The recent study of Bose-Einstein effects is of special interest for several reasons. First, they may have an impact on W-mass measurements ([3] and references therein) in the four-jet channel ($W^+W^- \to q\bar{q}q\bar{q}$) where the space-time regions of hadronization of the two W's overlap. This is due to the fact that the experimentally observed radius of the hadron-emission source is of order 1 fm, 10 times the distance between the W^+W^- decay vertices. A second reason is that the actual shape and width of the correlation function reflects the shape and size of the space-time region over which particle production occurs. Measurements of Bose-Einstein effects therefore directly test our understanding of QCD.

So far no appropriate theory exists which can describe the process of hadron production (or parton fragmentation) in general and Bose-Einstein effects in particular. To arrive at any understanding of these phenomena, studies have been done of identical-boson correlations in e^+e^- collisions at LEP energies in terms of the invariant four-momentum difference Q of pairs of particles, and even using two- and three-dimensional distributions in components of Q. The shape of the correlation function in more than one dimension has been a major subject of theoretical study in recent years [4–9].

In this work, an analysis of the Bose-Einstein correlation function in the electron-positron annihilation process $e^+e^- \to Z \to$ hadrons is presented. Two-particle correlations of like-charged particles are studied as a function of two components of the four-momentum difference Q, in different transverse mass ranges. This analysis is similar to that of [10]. Not only a full data sample is considered, but also a two-jet sample.

2 The Bose-Einstein Correlation Function

The two-particle correlation function R'_2 of two particles having four momenta p_1 and p_2 is given by

$$R'_2(p_1, p_2) = \frac{\rho(p_1, p_2)}{\rho(p_1)\rho(p_2)} \tag{1}$$

where $\rho(p_1, p_2)$ is the two-particle probability density and $\rho(p_1)$ and $\rho(p_2)$ are the single-particle probability densities.

Since we are interested only in the correlations due to Bose-Einstein interference, the product of single-particle densities is replaced by $\rho_0(p_1, p_2)$, the two-particle density that would occur in the absence of Bose-Einstein correlations. Thus,

$$R_2 = \frac{\rho(p_1, p_2)}{\rho_0(p_1, p_2)} \tag{2}$$

measures the additional correlation due to Bose-Einstein interference. In practice, the 'reference sample' leading to ρ_0 is difficult to construct since it does not occur in nature.

As mentioned above, the actual shape of the enhancement curve reflects the space-time distribution of the boson source. In particular, if $f(x)$ is the space-time distribution of the source, $R_2(p_1, p_2)$ takes the form

$$R_2(p_1, p_2) = 1 + |G[f(x)]|^2 \tag{3}$$

where

$$G[f(x)] = \int f(x)\, e^{-i(p_1-p_2)x}\, \mathrm{d}x \tag{4}$$

is the Fourier transform of $f(x)$. Using the common simple assumption [1] of a Gaussian shape for the space-time distribution of the boson source, the function G in the correlation function is also a Gaussian.

3 Charged-Particle Selection

The data used in the analysis were collected by the L3 detector [11] in 1994 at the center-of-mass energy of $\sqrt{s} \simeq 91.2$ GeV. Data selection uses information on charged particles from the Time Expansion Chamber (TEC) and the Silicon Microvertex Detector (SMD) [11]. To make sure that events lie within the full acceptance of the TEC and SMD, we require

$$|\cos\theta_{\mathrm{thr}}| < 0.7 \tag{5}$$

where $\cos\theta_{\mathrm{thr}}$ is the polar angle of the thrust axis determined from charged tracks only.

To obtain a data sample with well reconstructed tracks, the following cuts are applied on charged tracks [12]

- TEC contains 62 wires, so that a particle passing through the wire chamber can produce a maximum of 62 hits. A charged track candidate is required to have at least 40 hits.
- A particle track is reconstructed by combining hits. However, it can happen that a track is combined from hits belonging to different particles. Therefore, by requiring the length of a track in terms of hits (the so-called 'span') to be at least 50, these mis-constructed tracks are rejected.
- The distance of closest approach (projected onto the transverse plane) of a track to the nominal interaction vertex is required to be less than 5 mm. This cut helps to correctly identify hadrons produced in the given reaction.
- The transverse momentum of a track must be larger than 100 MeV, otherwise it would not be measured accurately in TEC.

In order to reduce background arising from beam-gas, beam-wall interaction events and from leptonic events, we use the following selection criteria

$$\frac{\sum_i |\vec{p}_i|}{\sqrt{s}} > 0.15, \quad \frac{|\sum_i p_{\|i}|}{\sum_i |\vec{p}_i|} < 0.75, \quad \frac{|\sum_i \vec{p}_{\perp i}|}{\sum_i |\vec{p}_i|} < 0.75, \quad N_{\mathrm{ch}} > 4 \tag{6}$$

where $\vec{p}_i$ is the momentum of particle i, with components $p_{\|i}$ parallel to the beam direction and $\vec{p}_{\perp i}$ in the plane perpendicular to the beam direction, and where the sum runs over all tracks of an event. $N_{\rm ch}$ is the number of charged-particle tracks.

For the computation of the four-momentum difference Q, the resolution of the angle between pairs of tracks is of crucial importance, especially for small Q-values. For this reason we impose additional quality cuts on track resolution, which results in rejection of about 28% of the tracks. With this selection, good agreement is obtained between data and simulation of the difference in azimuthal as well as polar angle between pairs of tracks [13].

A total of about a million events satisfy all the selection criteria.

Part of the analysis is restricted to two-jet events defined as events with a thrust value of more than 0.95 [2)]. In this way, the thrust axis is a good measure for the jet axis (or the longitudinal axis).

4 The Analysis

Since the mass of the two identical particles of the pair is fixed, the correlation function is defined in 6-dimensional momentum space. In practice, the correlation is large at small four-momentum difference $Q = \sqrt{-(p_1 - p_2)^2}$, so that often Bose-Einstein correlations are parametrized in this one-dimensional distance measure. There is no reason, however, to expect the hadron source to be spherically symmetric in jet fragmentation. This is the reason for performing a two-dimensional (parallel and transverse to thrust axis) analysis.

In our analysis we use the longitudinally comoving system (LCMS) [7]. This is defined for each pair of particles as the system in which the sum of the momenta of the pair is perpendicular to the thrust axis (which from here on is defined as the longitudinal direction). In other words, each pair of particles is Lorentz boosted to the system in which its rapidity vanishes. To see the advantage of this system we resolve the three-momentum difference of the pair of particles into a component $Q_{\|}$ parallel to the thrust axis, $Q_{\rm out}$ along to the sum of the particles' momenta and $Q_{\rm side}$ perpendicular to both $Q_{\|}$ and $Q_{\rm out}$. Doing so, one can write the invariant four-momentum difference as [14]

$$Q^2 = Q_{\|}^2 + Q_{\rm side}^2 + Q_{\rm out}^2(1-\beta^2) \tag{7}$$

where

$$\beta \equiv \frac{p_{\rm t1} + p_{\rm t2}}{E_1 + E_2} \tag{8}$$

with $p_{{\rm t}i}$ and E_i ($i = 1, 2$) the transverse momenta and energies of the particles in the LCMS. Thus, the energy difference and therefore the difference in emission time of the

[2)] The thrust is defined as the sum of the lengths of the longitudinal momenta of the final state particles relative to the axis $\vec{n}_{\rm thr}$ which maximizes the sum: $T = \max \frac{\sum_i |\vec{p}_i \cdot \vec{n}_{\rm thr}|}{\sum_i |\vec{p}_i|}$, where i runs over all the final state particles. For a two-jet event $T \simeq 1$, for an isotropic event $T \simeq 1/2$.

particles couples only to the component Q_{out}. In the present analysis we take the out and side directions together into a two-dimensional vector

$$\vec{Q}_{\perp} \equiv (Q_{\text{out}}, Q_{\text{side}}) \tag{9}$$

and perform a two-dimensional analysis using $Q_{\parallel}$ and $|\vec{Q}_{\perp}|$. The three dimensional analysis is left for the future.

The correlation function R_2 (equation (2)) is measured as a function of $Q_{\parallel}$ and $|\vec{Q}_{\perp}|$ by counting the number of like-sign pairs in bins of these variables for both the data and a 'reference sample'. The reference sample is formed by mixing particles from different events in the following way. First events are stored in a 'pool'. Then events are randomly selected from this pool and their tracks replaced by tracks from other events in the pool under the condition that no tracks originate from the same event, and $Q_{\parallel}$ and $|\vec{Q}_{\perp}|$ are calculated for each pair.

In this algorithm the pairs are uncorrelated. However, the mixing procedure removes more correlations than just those of Bose-Einstein, e.g., those from energy-momentum conservation and from resonances. This effect is estimated by Monte Carlo (MC) using a generator with no Bose-Einstein effects (JETSET [15] or HERWIG [16]), which has been tuned to reproduce event-shape distributions [17]. Thus, in the absence of Bose-Einstein correlations, the corrected two-particle density is

$$\rho_0(p_1, p_2) = \rho_{\text{mix}} \cdot \left[\frac{\rho}{\rho_{\text{mix}}}\right]_{\text{MC,noBE}} \tag{10}$$

The two-particle density of the data must be corrected for detector resolution, acceptance and efficiency. This is done bin-by-bin by multiplying the values obtained from the raw data by a correction factor. To determine this factor, events generated by Monte Carlo are passed through the L3 detector simulation program [18], reconstructed and subjected to track and event selection in the same way as the data. The correction factor is then the ratio of the density found from the generator MC to that found from the reconstructed and selected MC data. This correction factor was determined using event samples generated by JETSET (with and without BE) and HERWIG.

In terms of numbers of like-sign particle pairs, R_2 is given, for bin m, n of $Q_{\parallel}$, $|\vec{Q}_{\perp}|$, by

$$R_{2\,mn} = \left[\frac{N_{mn}}{N_{mn}^{\text{mix}}}\right]_{\text{raw}} \cdot \left[\frac{N_{mn}^{\text{mix}}}{N_{mn}}\right]_{\text{MC,noBE}} \cdot \left[\frac{N_{mn}^{\text{gen}}}{N_{mn}^{\text{det}}}\right]_{\text{MC}} \tag{11}$$

where N_{mn} is the normalized number of pairs in the bin.

Assuming a Gaussian shape for the source, we arrive at the following two-dimensional parametrization:

$$R_2(Q_{\parallel}, \vec{Q}_{\perp}) = \gamma \left(1 + \delta Q_{\parallel} + \varepsilon|\vec{Q}_{\perp}|\right) \left[1 + \lambda \exp\left(-R_{\parallel}^2 Q_{\parallel}^2 - R_{\perp}^2 \vec{Q}_{\perp}^2\right)\right] \tag{12}$$

where the factor $(1 + \delta Q_{\parallel} + \varepsilon|\vec{Q}_{\perp}|)$ takes into account possible long-range momentum correlations in the form of a slow rise, γ is a normalization factor and λ is the incoherence factor which measures the strength of the correlation. By fitting the correlation function with this parametrization, one can extract the incoherence factor λ and the radii $R_{\|}$ and $R_{\perp}$. The parameter $R_{\|}$ is usually interpreted as the longitudinal geometric radius of the boson emitting source, while $R_{\perp}$ measures a mixture of the transverse radius and emission time.

R_2 depends not only on the momentum difference but also on the sum, c.f. equation (8). We therefore investigate the dependence of λ, $R_{\|}$ and $R_{\perp}$ on the avarage transverse mass $m_{\mathrm{T}} = \frac{1}{2}[(m^2+p_{\mathrm{t1}}^2)^{1/2} + (m^2+p_{\mathrm{t2}}^2)^{1/2}]$ of the pair of like-charged particles. It has been suggested that λ increases and the radii decrease when m_{T} increases [14].

As a check of the method we performed the analysis using events generated by JETSET without BE at detector level instead of the experimental data. Fig. 1 shows the results for all events when the correction factor is determined using JETSET with BE and the reference sample using JETSET without BE. A two-dimensional histogram of R_2 is shown as a function of $Q_{\|}$ and $|\vec{Q}_{\perp}|$ as well as slices in different intervals of $Q_{\|}$ and $|\vec{Q}_{\perp}|$. Fits give results consistent with $\lambda = 0$, as expected if there are no Bose-Einstein correlations. The fit results are also in good agreement with $\lambda = 0$ when we take two-jet events and when the sample is divided into different m_{T} intervals. The same checks were performed (a) using HERWIG to determine the correction factor and (b) using HERWIG to determine the reference sample and JETSET (with or without BE) to determine the correction factor. In all cases the results are consistent with no Bose-Einstein correlations.

5 The Results

We have used three different Monte Carlo generators (JETSET with and without BE and HERWIG) to determine the correction factors and two generators (JETSET without BE and HERWIG) to compute the reference sample (equation (10)) to determine the correlation funcion R_2 of (11) in six different ways.

Fig. 2a shows a two-dimensional histogram of R_2 as a function of $Q_{\|}$ and $|\vec{Q}_{\perp}|$ for all data when the correction factor is determined using JETSET with BE and the reference sample using JETSET without BE. The parametrization (12) is fitted to this two-dimensional histogram. The results of the fit are shown in the first line of table 1. Also shown in the figure are slices in different intervals of $Q_{\|}$ and $|\vec{Q}_{\perp}|$ together with curves resulting from the fit. In fig. 2b the correction factor is determined using JETSET without BE.

Figures 3a and 3b show analogous plots for two-jet events. The fit results are given in the first line of table 2.

The fit results for λ, $R_{\|}$ and $R_{\perp}$ of all six computations are shown in fig. 4 for all data as well as for two-jet events. From this figure it is clear (a) that there is no significant difference between the results obtained from all data and the results obtained from two-jet events and (b) that $R_{\|}$ is significantly larger than $R_{\perp}$. This feature is theoretically predicted in [4]: it suggests a longitudinal stretching of the string field.

Another feature is that the parameters are in general larger when the HERWIG Monte

Carlo is used in the reference sample than when JETSET without BE is used.

In general, the fits using JETSET with BE to determine correction factors and using JETSET without BE for the reference distribution have the best chi-squared. Therefore, we take the results from these fits as the best values of the parameters. As systematic error we take the RMS of the values obtained from the six different computations. This corresponds to the second errors given in table 1.

In table 1 results are also shown for different ranges of m_{T}, in order to look for a possible increase of the λ parameter and decrease of the radii $R_{||}$ and $R_{\perp}$ when m_{T} increases [14]. Table 2 gives analogous results for two-jet events. Again, no significant differences are seen between the results obtained for all data and those obtained for two-jet events. The value of $R_{||}$ is always larger than the value of $R_{\perp}$, also in different regions of m_{T}. The expected increase of λ with increasing m_{T} can not be confirmed. However, a general decrease of $R_{||}$ and $R_{\perp}$ is observed when m_{T} increases. This behavior of the radii with respect to m_{T} is seen separately for all six computations (not shown).

A possible explanation [10] for the decrease of $R_{||}$ when m_{T} increases is that resonances propagate out of the primary hadron source, since resonances travel some distance before they decay. Assuming that resonaces and non-resonant particles are produced with approximately the same momentum distribution, the particles coming from resonances have relatively low momenta. Consequently, there are more particles coming from resonances in low-m_{T} than in high-m_{T} pairs. Effectively, the source therefore decreases towards high m_{T} values. By the same argument one would expect λ to be smaller for small m_{T}. For a similar explanation of the decrease of $R_{\perp}$ with m_{T} one has to be very careful, since $R_{\perp}$ measures a mixture of the transverse radius and the emission time.

6 Summary

An analysis was performed of the Bose-Einstein correlation function in the electron-positron annihilation process $\mathrm{e^+e^-} \to \mathrm{Z^0} \to$ hadrons at LEP. Two-particle correlations of like-charged particles were studied in two dimensions (parallel and transverse to the thrust axis) in the longitudinally comoving system. Using the parametrization (12) we extracted the incoherence factor λ and the radii $R_{||}$ and $R_{\perp}$ for both the full data sample and for a two-jet sample. These parameters were also measured for different intervals of the average transverse mass of the pion pair.

No significant difference was found between the results for all data and those for two-jet events. For all data we found $\lambda = 0.30 \pm 0.01 \pm 0.07$, $R_{||} = 0.73 \pm 0.02 \pm 0.04\,\mathrm{fm}$ and $R_{\perp} = 0.54 \pm 0.02 \pm 0.05\,\mathrm{fm}$. The value of $R_{||}$ is always larger than that of $R_{\perp}$, also in different regions of m_{T}. Furthermore, our data do not confirm a possible increase of λ with increasing m_{T}. However, a decrease is seen in the radii $R_{||}$ and $R_{\perp}$ when m_{T} increases.

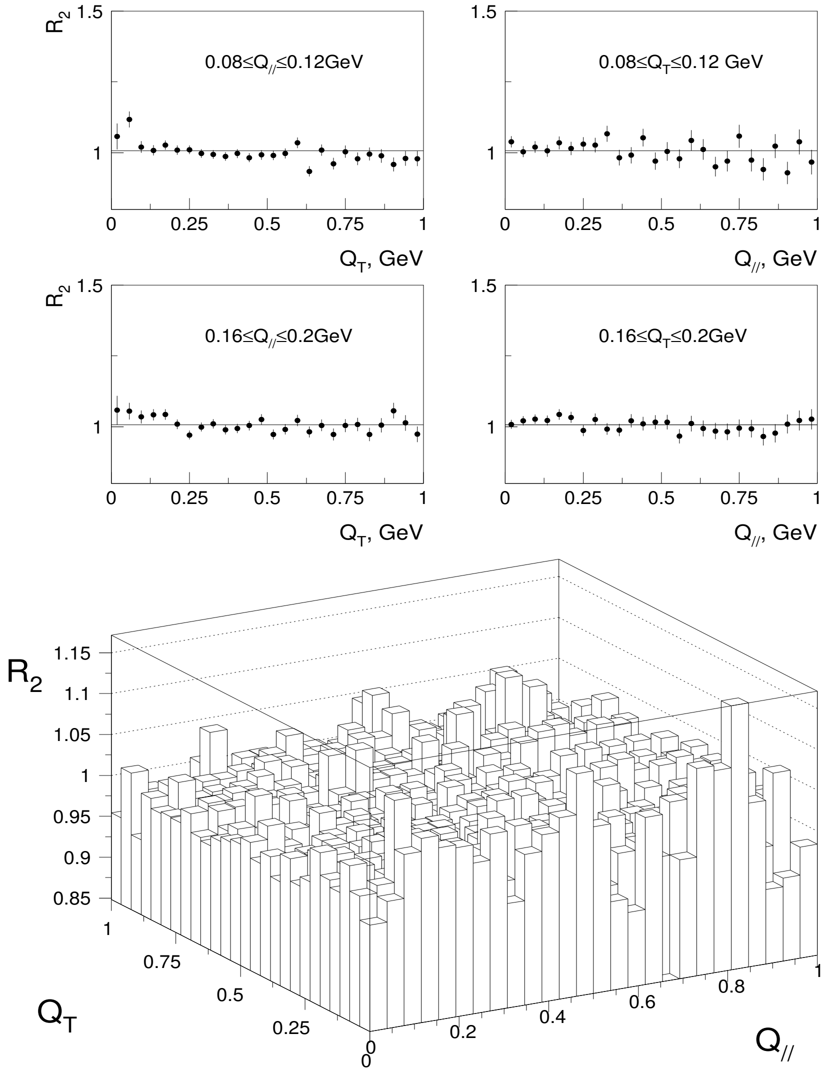

Figure 1: R_2 as a function of $Q_{\parallel}$ and $|\vec{Q}_{\perp}|$ for all JETSET simulated events when no BE effects are included. The correction factor is determined by JETSET with BE and the reference distribution by JETSET without BE.

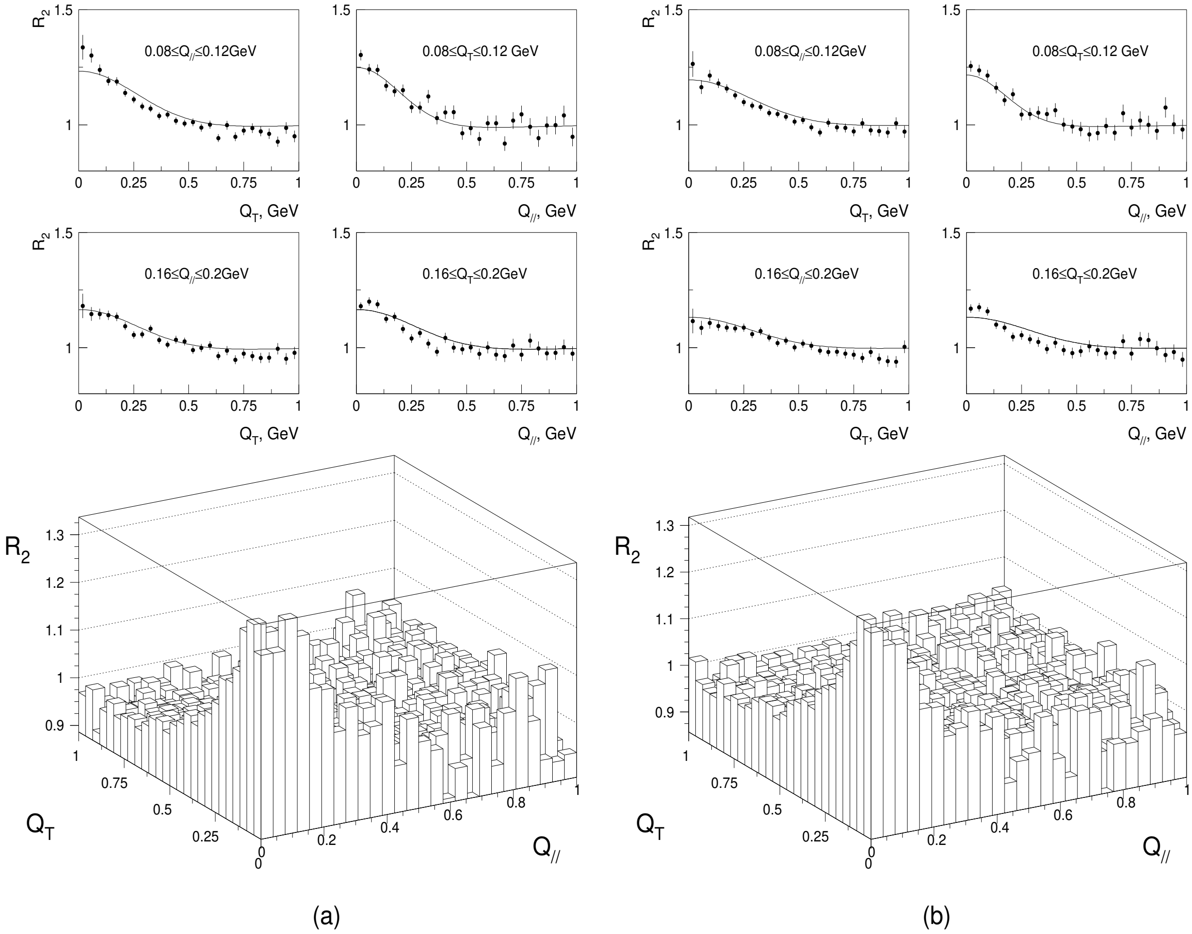

Figure 2: R_2 as a function of $Q_\parallel$ and $|\vec{Q}_\perp|$ for all data when the correction factor is determined using JETSET with BE (a) and without BE (b). The reference distribution is from JETSET without BE.

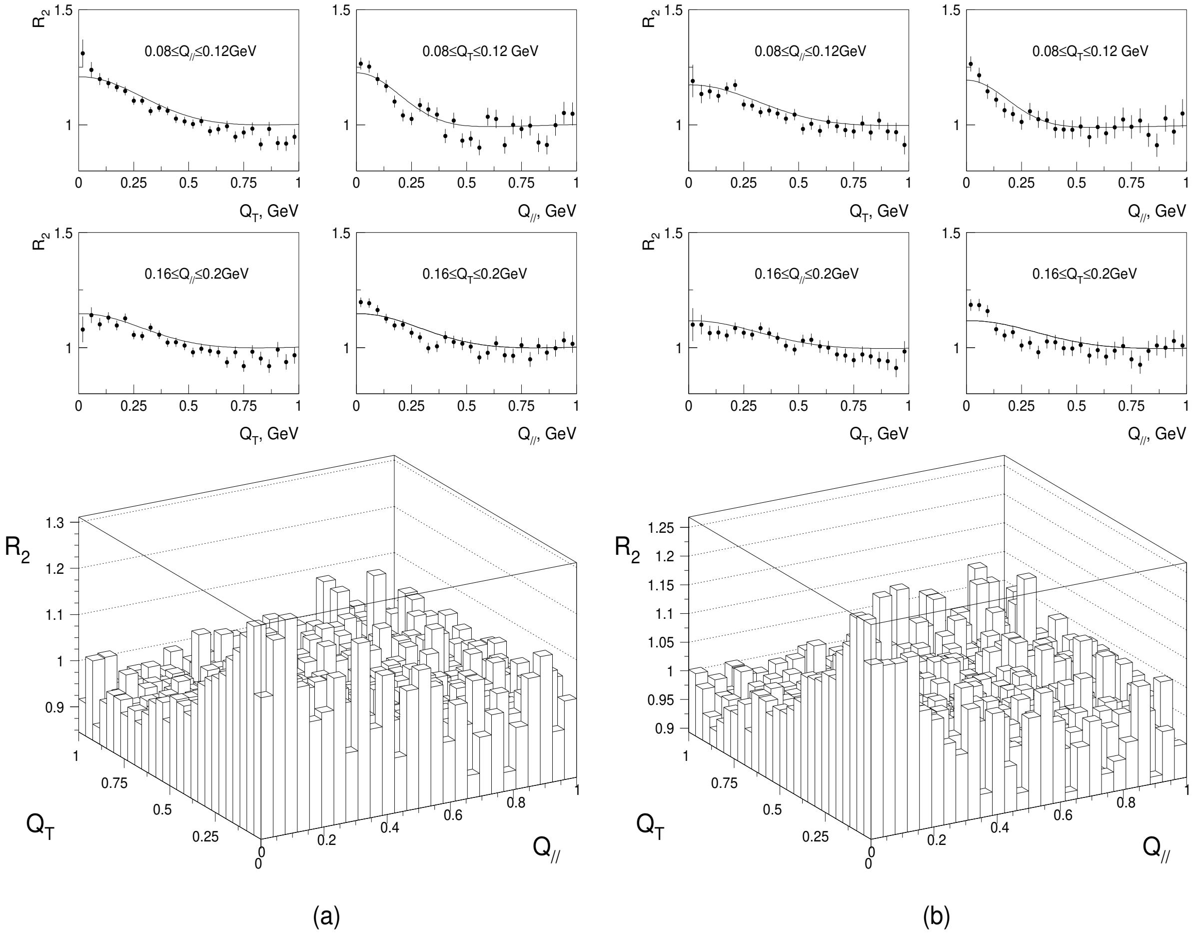

Figure 3: R_2 as a function of $Q_{\parallel}$ and $|\vec{Q}_{\perp}|$ for two-jet events when the correction factor is determined using JETSET with BE (a) and without BE (b). The reference distribution is from JETSET without BE.

Table 1: Values of the fit parameters for all data

range (GeV)	λ	$R_{\parallel}$(fm)	$R_{\perp}$(fm)
total	$0.30 \pm 0.01 \pm 0.07$	$0.73 \pm 0.02 \pm 0.04$	$0.54 \pm 0.02 \pm 0.05$
$0.14 < m_{\rm T} < 0.30$	$0.30 \pm 0.02 \pm 0.06$	$0.76 \pm 0.05 \pm 0.08$	$0.72 \pm 0.04 \pm 0.04$
$0.30 < m_{\rm T} < 0.45$	$0.40 \pm 0.02 \pm 0.06$	$0.70 \pm 0.04 \pm 0.02$	$0.51 \pm 0.03 \pm 0.03$
$m_{\rm T} > 0.45$	$0.35 \pm 0.03 \pm 0.06$	$0.63 \pm 0.04 \pm 0.04$	$0.38 \pm 0.02 \pm 0.02$

Table 2: Values of the fit parameters for two-jet events

range (GeV)	λ	$R_{\parallel}$(fm)	$R_{\perp}$(fm)
total	$0.28 \pm 0.02 \pm 0.09$	$0.72 \pm 0.03 \pm 0.06$	$0.49 \pm 0.02 \pm 0.05$
$0.14 < m_{\rm T} < 0.30$	$0.25 \pm 0.03 \pm 0.07$	$0.77 \pm 0.07 \pm 0.10$	$0.58 \pm 0.05 \pm 0.04$
$0.30 < m_{\rm T} < 0.45$	$0.38 \pm 0.03 \pm 0.04$	$0.71 \pm 0.05 \pm 0.05$	$0.50 \pm 0.03 \pm 0.03$
$m_{\rm T} > 0.45$	$0.32 \pm 0.04 \pm 0.09$	$0.55 \pm 0.07 \pm 0.07$	$0.38 \pm 0.03 \pm 0.01$

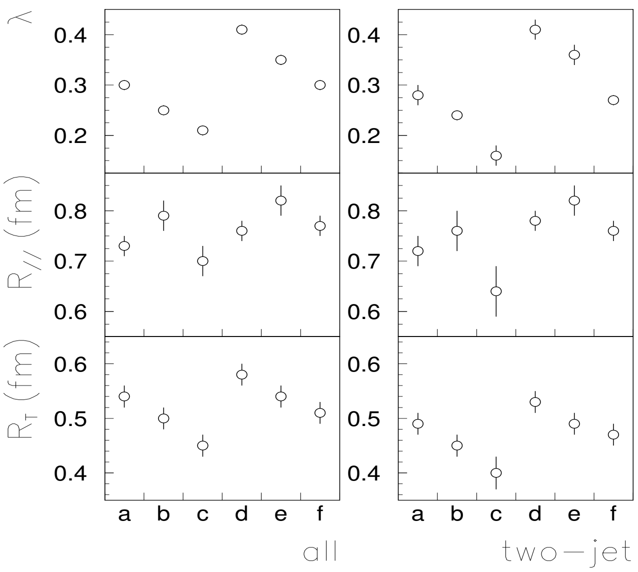

Figure 4: Fit results of the parametrization for all data and for two-jet events when the correction factor and the reference sample are determined by (a): JETSET with BE, JETSET without BE, (b): JETSET without BE, JETSET without BE, (c): HERWIG, JETSET without BE, (d): JETSET with BE, HERWIG, (e): JETSET without BE, HERWIG, (f): HERWIG, HERWIG.

References

[1] G. Goldhaber, S. Goldhaber, W. Lee and A. Pais, Phys. Rev. Lett. **3** (1959) 181.

[2] D.H. Boal, C.K. Gelbke, B.K. Jennnings, Rev. Mod. Phys. **62** (1990) 553.

[3] L. Lönnblad and T. Sjöstrand, Phys. Lett. **B351** (1995) 293 and Eur. Phys. J. **C2** (1998) 165.

[4] B. Andersson, M. Ringnér, Transverse and Longitudinal Bose-Einstein Correlation, Univ. of Lund preprint HEP-PH/9710334.

[5] G. Bertsch, M. Gong and M. Tohyama, Phys. Rev **C37** (1988) 1896.

[6] S. Pratt, T.Csösgő and J. Zimanyi, Phys. Rev. **C42** (1990) 2646.

[7] J.D. Bjorken, Phys. Rev. **D27** (1983) 140.

[8] U. Heinz et al., Phys. Lett. **B382** (1996) 181.

[9] F. Yano and S. Koonin, Phys. Lett. **B78** (1978) 556; M. Podgoretskiĭ, Sov. J. Nucl. Phys. **37** (1983) 272.

[10] B. Lörstad, O.G. Smirnova, Transverse Mass Dependence of Bose-Einstein Correlation Radii in e^+e^- annihilation at LEP Energies, Proc. 7^{th} Int. Workshop on Multiparticle Production "Correlations and Fluctuations", Nijmegen 1996, Eds.: R.C. Hwa et al. (World Scientific, Singapore **A57**) p. 42.

[11] L3 Collab., B. Adeva et al., Nucl. Inst. Meth. **A289** (1990) 35; J.A. Bakken et al., Nucl. Inst. Meth. **A275** (1989) 81; O. Adriani et al., Nucl. Inst. Meth. **A302** (1991) 53; B. Adeva et al., Nucl. Inst. Meth. **A323** (1992) 109; K. Deiters et al., Nucl. Inst. Meth. **A323** (1992) 162; B. Acciari et al., Nucl. Inst. Meth. **A351** (1994) 300.

[12] S.V. Chekanov, "Local Multiplicity fluctuations and Intermittent Structure inside Jets", Ph.D. Thesis, Univ. of Nijmegen, The Netherlands (1997) ISBN 90-9010518-2.

[13] M. Acciarri et al. (L3 Collaboration), Local Multiplicity Fluctuations in Hadronic Z-decays, CERN-PPE/97-165, submitted to Phys. Lett. B.

[14] R. Mueşan, O.G. Smirnova, B. Lörstad, On the m_{T} Dependence of the Bose-Einstein Effect, Univ. of Lund preprint LUNFD 6/NFFL-7149, 1997.

[15] T. Sjöstrand, Comp. Phys. Comm. **82** (1994) 74.

[16] G. Marchesini and B.R. Webber, Nucl. Phys. **B310** (1988) 461, G. Marchesini et al., Comp. Phys. Comm. **67** (1992) 465.

[17] L3 Collab., B. Adeva et al., Z. Phys. **C55** (1992) 39.

[18] The L3 detector simulation is based on GEANT3, see R. Brun et al., CERN report CERN DD/EE/84-1 (Revised), 1987, and uses GHEISHA to simulate hadronic interactions, see H. Fesefeldt, RWTH Aachen report PITHA 85/02, 1985.